

WIDE-ANGLE REFLECTION WAVE POLARIZERS USING INHOMOGENEOUS PLANAR LAYERS

M. Khalaj-Amirhosseini and S. M. J. Razavi

College of Electrical Engineering
Iran University of Science and Technology
Narmak, Tehran, Iran

Abstract—In this paper, inhomogeneous planar layers are optimally designed as reflection wave polarizers in a desired incidence angles range. First, the electric permittivity function of the structure is expanded in a truncated Fourier series. Then, the optimum values of the coefficients of the series are obtained through an optimization approach. The validation and the performance of the proposed structure are verified using some examples.

1. INTRODUCTION

Wave polarizers have found some applications in microwave and optical systems such as free-space optical switching networks, read-write magneto-optic data storage systems and polarization-based imaging systems [1–14]. In a wave polarizer only one of two possible modes (TE or TM) can be appeared in the transmission or reflection waves. One may classify polarizers into the following types [9, 14]: dichroic polarizers, anisotropic crystal polarizers, Brewster angle polarizers, wire-grid polarizers and gyrotropic slab polarizers. The most straightforward idea to design a wave polarizer is using the Brewster's angle to eliminate the TM mode in the reflection wave [8, 9]. However, the Brewster's polarizers work only at a narrow range of angles of incidence. On the other hand, Inhomogeneous Planar Layers (IPLs) are widely used in microwave and antenna engineering [15–19]. In this paper, we propose utilizing IPLs as reflection wave polarizers in a desired incidence angles range. To optimally design IPLs, their electric permittivity function is expanded in a truncated Fourier series, first. Then, the optimum values of the coefficients of the series are

Corresponding author: M. Khalaj-Amirhosseini (khalaja@iust.ac.ir).

obtained through an optimization approach. The identical procedure has been used to optimally design IPLs as Radomes [18] and impedance matchers between two different mediums [19] previously. Finally, the usefulness of the proposed structure is verified using some examples.

2. ANALYSIS OF IPLS

In this section, the frequency domain equations of the IPLs are reviewed. Fig. 1 shows a typical IPL with thickness d , whose left and right mediums are the free space and whose electric permittivity function is $\varepsilon_r(z)$. One way to fabricate the IPLs is to place several thin homogeneous dielectric layers beside each other. It is assumed that the incidence plane wave propagates obliquely towards positive x and z direction with an angle of incidence θ_i and electric field strength E^i . Also, two different polarizations are possible, one is the TM and the other is the TE. We desire to design the introduced polarizer so that only TE mode is reflected to the input medium, i.e., $z < 0$, and TM mode can't be reflected.

The differential equations describing IPLs have non-constant coefficients and so except for a few special cases no analytical solution exists for them. There are some methods to analyze the IPLs such as cascading many short sections [20], Finite Difference [21], Taylor's Series Expansion [22], Fourier Series Expansion [23], the Equivalent Sources Method [24], the Method of Moments [25] and an approximate closed form solution [26]. Almost in all of these methods, the IPLs are modeled as a nonuniform transmission line with the following

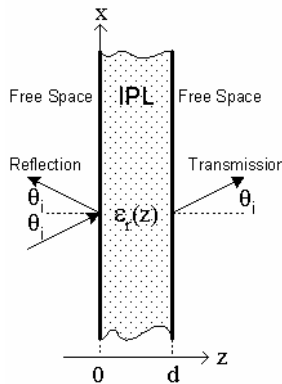


Figure 1. A typical IPL as a reflection wave polarizer.

characteristic impedance and propagation coefficient

$$Z_c(z) = \begin{cases} \frac{\eta_0}{\sqrt{\varepsilon_r(z) - \sin^2(\theta_i)}}, & \text{TE} \\ \frac{\eta_0}{\varepsilon_r(z)} \sqrt{\varepsilon_r(z) - \sin^2(\theta_i)}, & \text{TM} \end{cases} \quad (1)$$

$$\beta = \frac{2\pi}{\lambda_t} = \frac{\omega}{c} \sqrt{\varepsilon_r(z) - \sin^2(\theta_i)} \quad (2)$$

where c is the velocity of the light, λ_t is the transverse wavelength and η_0 is the wave impedance in the free space. After finding the $ABCD$ parameters of the equivalent nonuniform transmission lines [20–26], the input reflection coefficient will be determined as follows

$$\Gamma = \frac{(A - \eta_{0t}C) \eta_{0t} + (B - \eta_{0t}D)}{(A + \eta_{0t}C) \eta_{0t} + (B + \eta_{0t}D)} \quad (3)$$

where

$$\eta_{0t} = \begin{cases} \frac{\eta_0}{\cos(\theta_i)}, & \text{TE} \\ \eta_0 \cos(\theta_i), & \text{TM} \end{cases} \quad (4)$$

is the transverse impedance of the free space.

It is well known that a high performance reflection polarizer has to operate over a wide range of incidence angles, the extinction ratio of the unwanted to the desired polarized wave in reflection is small and the reflectance for the desired polarization is high. Hence to show the performance of a polarizer, we define the extinction ratio R_Γ as the ratio of reflection coefficient of TM mode to that of TE mode, as follows

$$R_\Gamma \triangleq \frac{\Gamma_{\text{TM}}}{\Gamma_{\text{TE}}} \quad (5)$$

It is evident that as R approaches zero the performance of the polarizer becomes better. Moreover, a good polarizer should have TE reflection coefficient $|\Gamma_{\text{TE}}|$ as higher as possible.

3. SYNTHESIS OF POLARIZERS

In this section, a general method is proposed to optimally design the IPLs as polarizers. First, we consider the following truncated Fourier series expansion for the electric permittivity function

$$\ln(\varepsilon_r(z) - 1) = \sum_{n=0}^N C_n \cos(\pi n z / d) \quad (6)$$

To enforce the designed polarizers to be symmetric, we have to use the following truncated Fourier series instead of (6) for the electric permittivity function.

$$\ln(\varepsilon_r(z) - 1) = \sum_{n=0}^N C'_n \cos(2\pi n z/d) \quad (7)$$

An optimum designed polarizer has to have a parameter R_Γ defined in (5) as small as possible in a desired incidence angle range, while the amplitude of the reflected TE mode is being constant at that range. Therefore, the optimum values of the coefficients C_n in (6) or C'_n in (7) can be obtained through minimizing the following error function corresponding to J incidence angles between $\theta_{i,\min}$ and $\theta_{i,\max}$.

$$\begin{aligned} \text{Error} = & \sqrt{\frac{1}{J} \sum_{j=1}^J |R_\Gamma(\theta_i^{(j)})|^2} \\ & + \sqrt{\frac{1}{J} \sum_{j=1}^J |R_\Gamma(\theta_i^{(j)})|^2 - \left(\frac{1}{J} \sum_{j=1}^J |R_\Gamma(\theta_i^{(j)})|\right)^2} \\ & + \sqrt{\frac{1}{J} \sum_{j=1}^J |\Gamma_{\text{TE}}(\theta_i^{(j)})|^2 - \left(\frac{1}{J} \sum_{j=1}^J |\Gamma_{\text{TE}}(\theta_i^{(j)})|\right)^2} \quad (8) \end{aligned}$$

The second and third terms in (8) act as variance functions to keep constant $|R_\Gamma|$ and $|\Gamma_{\text{TE}}|$, respectively, in desired incidence angles range. Moreover, defined error function should be restricted by some constraints such as easy fabrication given by

$$\max\{\varepsilon_r(z)\} \leq (\varepsilon_r)_{\max} \quad (9)$$

where $(\varepsilon_r)_{\max}$ is the maximum value of $\varepsilon_r(z)$, in the fabrication step.

4. EXAMPLES AND RESULTS

In this section we investigate and validate the capability of IPLs as wide-angle reflection wave polarizer. First of all, consider a homogeneous planar layer with permittivity $\varepsilon_r = 7.55$ as a polarizer operating at Brewster's angle $\theta_i = 70^\circ$. Figs. 2 and 3, illustrate the magnitude of TE and TM reflection coefficients and R_Γ versus the incidence angle for some thickness d . It is seen that the polarizers with thickness d equal to a quarter of transverse wavelength ($\lambda_t/4 = 5.81$ mm for $f = 10$ GHz) at Brewster's angle has the best performance,

i.e., more TE reflection. Importantly, it is seen that Brewster's polarizers operate at a very narrow incidence angle range. Now, we would like to design an IPL as a polarizer for incidence angles between $\theta_{i,\min} = 60^\circ$ and $\theta_{i,\max} = 80^\circ$ at frequency 10.0 GHz, considering $(\epsilon_r)_{\max} = 10$. Using the proposed optimization approach, considering $N = 10$ spatial harmonics and $J = 10$ incidence angles four polarizers were synthesized assuming their thickness to be $d = 5, 10, 20$ and

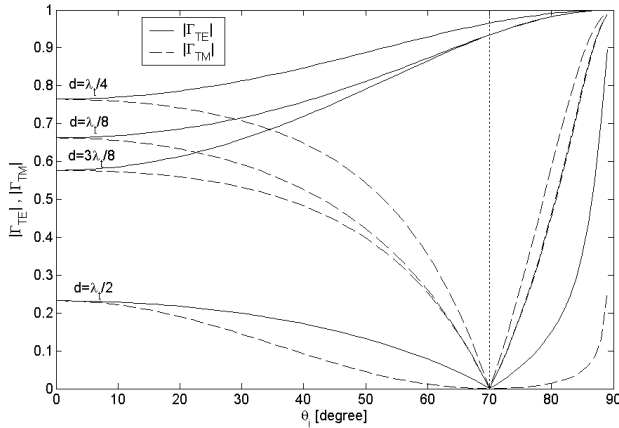


Figure 2. The $|\Gamma_{TE}|$ and $|\Gamma_{TM}|$ of homogeneous planar layer for $\theta_i = 70^\circ$.

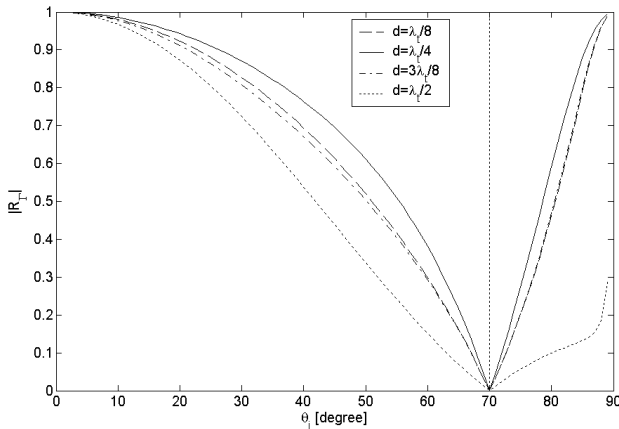


Figure 3. The $|R_\Gamma|$ of homogeneous planar layer for $\theta_i = 70^\circ$.

25 mm. The unknown coefficients of the truncated Fourier series related to the synthesized polarizers are written in Table 1. Fig. 4 illustrates the obtained electric permittivity function $\varepsilon_r(z)$ and Figs. 5 and 6 illustrate the magnitude of TE and TM reflection coefficients and R_Γ versus the incidence angle. It is observed that the designed polarizers have a low TM reflection at the incidence angle range of

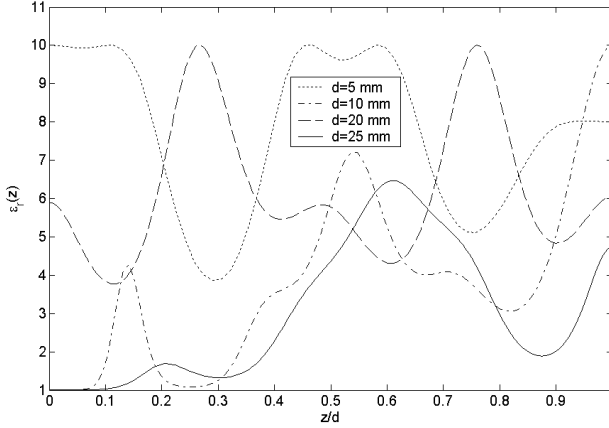


Figure 4. The electric permittivity function $\varepsilon_r(z)$ of polarizers Nos. 1–4 for $f = 10$ GHz, $(\varepsilon_r)_{\max} = 10$ and $\theta_i = [60^\circ, 80^\circ]$.

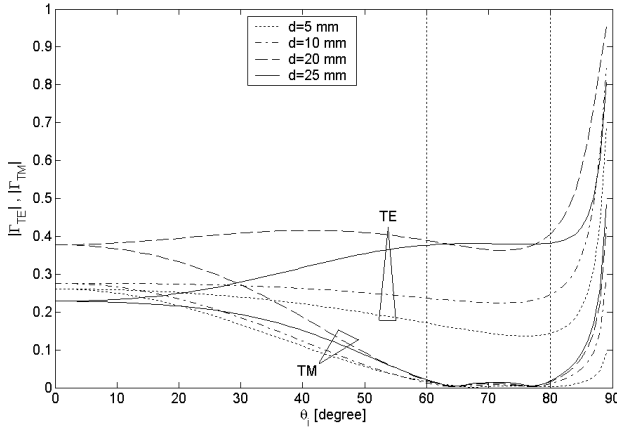


Figure 5. The $|\Gamma_{TE}|$ and $|\Gamma_{TM}|$ of polarizers Nos. 1–4 for $f = 10$ GHz, $(\varepsilon_r)_{\max} = 10$ and $\theta_i = [60^\circ, 80^\circ]$.

$\theta_i = [60^\circ, 80^\circ]$. Also, it is seen that as the thickness of polarizer is selected higher the magnitude of TE reflection is increased. Fig. 7 illustrates the $|\Gamma_{TE}|$, $|\Gamma_{TM}|$ and $|R_\Gamma|$ of the fifth polarizer versus the incidence angle considering $\theta_{i,\min} = 65^\circ$ and $\theta_{i,\max} = 75^\circ$ and $d = 25$ mm. Also, Fig. 8 illustrates the $|\Gamma_{TE}|$, $|\Gamma_{TM}|$ and $|R_\Gamma|$ of the sixth polarizer versus the incidence angle considering $\theta_{i,\min} = 40^\circ$

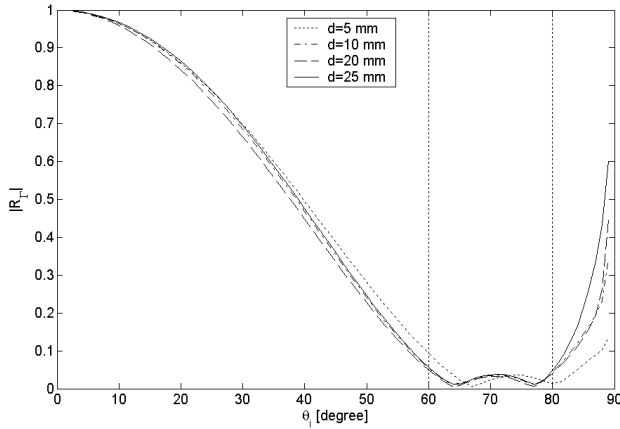


Figure 6. The $|R_\Gamma|$ of polarizers Nos. 1–4 for $f = 10$ GHz, $(\varepsilon_r)_{\max} = 10$ and $\theta_i = [60^\circ, 80^\circ]$.

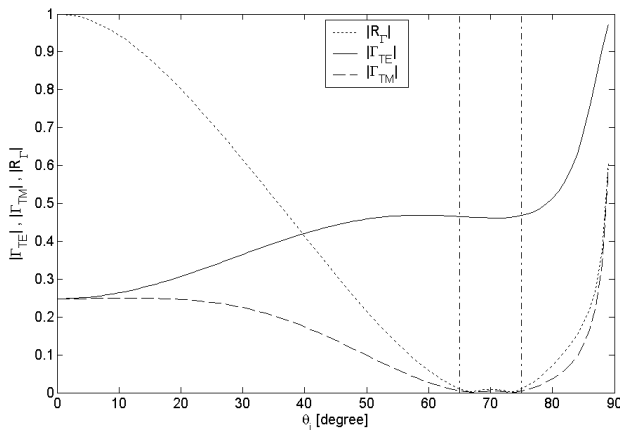


Figure 7. The $|\Gamma_{TE}|$, $|\Gamma_{TM}|$ and $|R_\Gamma|$ of polarizer No. 5 for $f = 10$ GHz, $(\varepsilon_r)_{\max} = 10$ and $\theta_i = [65^\circ, 75^\circ]$.

and $\theta_{i,\max} = 50^\circ$ and $d = 50$ mm. The obtained electric permittivity function and the unknown coefficients of the fifth and sixth polarizer are shown in Fig. 9 and Table 1, respectively. Comparing Figs. 5–8 with each other gives us that as the desired relative incidence angle

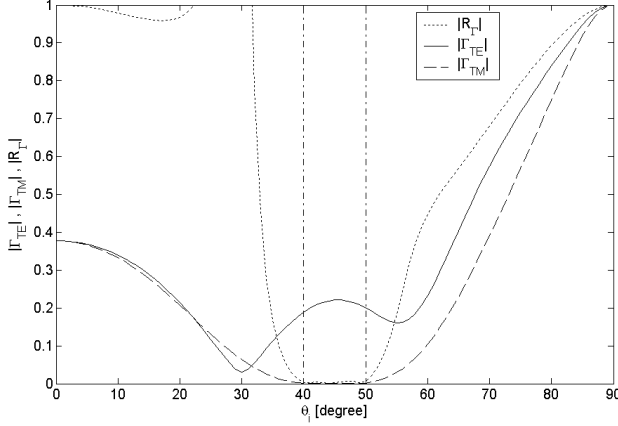


Figure 8. The $|\Gamma_{TE}|$, $|\Gamma_{TM}|$ and $|R_\Gamma|$ of polarizer No. 6 for $f = 10$ GHz, $(\varepsilon_r)_{\max} = 10$ and $\theta_i = [40^\circ, 50^\circ]$.

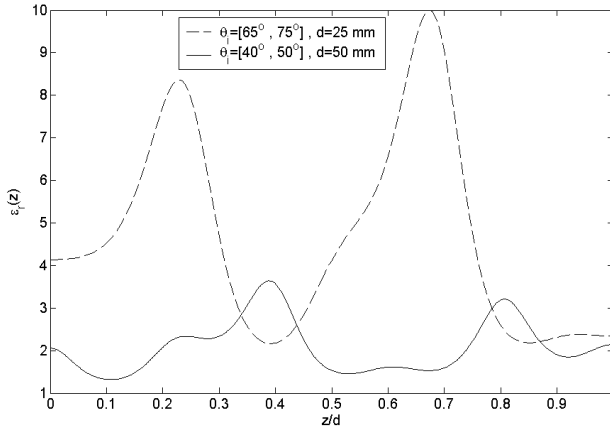


Figure 9. The electric permittivity function $\varepsilon_r(z)$ of polarizers Nos. 5 and 6 for $f = 10$ GHz and $(\varepsilon_r)_{\max} = 10$.

range defined by

$$w_\theta = 2 \frac{\theta_{i,\max} - \theta_{i,\min}}{\theta_{i,\max} + \theta_{i,\min}} \quad (10)$$

is decreased, the performance of the optimum designed polarizers is increased. It is an interesting result from Fig. 8 that IPLs can be designed as polarizers for the incidence angles smaller than 45°

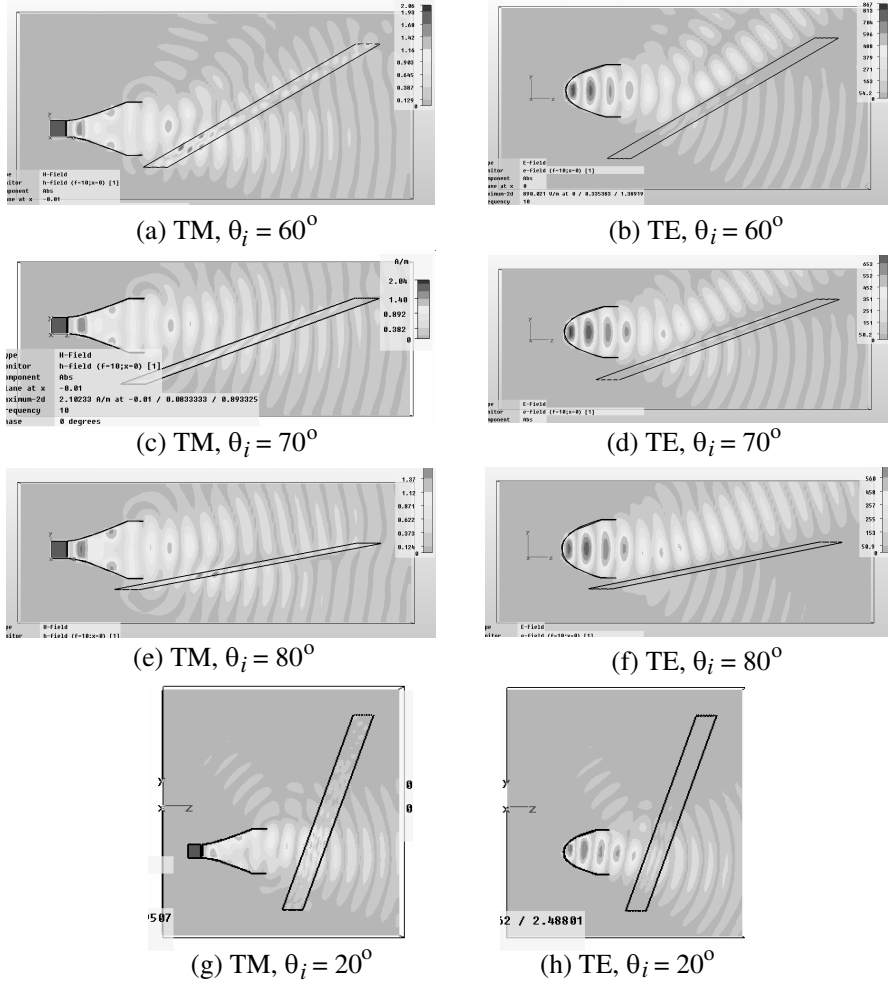


Figure 10. The absolute of electric and magnetic fields, respectively for TE and TM polarized incident wave at $f = 10$ GHz simulated by CST software.

Table 1. The unknown coefficients of the truncated Fourier series of designed polarizers for $f = 10$ GHz and $(\varepsilon_r)_{\max} = 10$.

	C_0	C_1	C_2	C_3	C_4	C_5	C_6	C_7	C_8	C_9	C_{10}
No. 1: $\theta_i = [60^\circ, 80^\circ]$ $d = 5$ mm	1.8507	0.0393	0.0233	0.1827	0.3856	-0.0736	-0.1329	-0.0869	-0.1186	0.0644	0.0630
No. 2: $\theta_i = [60^\circ, 80^\circ]$ $d = 10$ mm	0.1343	-2.0181	-1.1643	-0.5973	0.0014	-0.7970	-0.8416	-1.1245	-0.8847	-0.7573	-0.3421
No. 3: $\theta_i = [60^\circ, 80^\circ]$ $d = 20$ mm	1.5946	-0.0601	-0.0532	-0.1171	-0.2960	0.1169	0.0535	0.0505	0.2848	-0.0047	0.0193
No. 4: $\theta_i = [60^\circ, 80^\circ]$ $d = 25$ mm	-0.2138	-1.9839	-1.6099	-0.3694	-0.4457	-0.8304	-0.3940	-0.5373	0.0367	-0.0525	0.1681
No. 5: $\theta_i = [65^\circ, 75^\circ]$ $d = 25$ mm	1.1038	0.3199	-0.2037	0.5110	-0.3513	-0.5141	0.1022	-0.0151	0.1746	0.1245	-0.1092
No. 6: $\theta_i = [40^\circ, 50^\circ]$ $d = 50$ mm	-0.0713	-0.1339	-0.0598	-0.4712	-0.2562	0.4220	0.0738	0.0795	0.0561	0.0647	0.3503

(despite low reflectivity of TE polarization), which it is not possible for Brewster's polarizers.

To validate the results, the performance of the designed polarizer No. 3 is simulated by full wave simulator CST software. Fig. 10 illustrate the absolute of electric and magnetic fields for TE and TM polarized incident wave, respectively, considering $f = 10$ GHz and $\theta_i = 20^\circ, 60^\circ, 70^\circ$ and 80° . It is seen the reflection of TM wave is nearly equal to that of TE wave at $\theta_i = 20^\circ$, while the reflection of TM wave is very weaker than that of TE wave at $\theta_i = 60^\circ, 70^\circ$ and 80° . Therefore, Fig. 10 is in agreement with Fig. 5 assuming $d = 20$ mm.

5. CONCLUSION

Inhomogeneous Planar Layers (IPLs) were optimally designed as reflection wave polarizers in a desired incidence angles range. First, the electric permittivity function of the structure is expanded in a truncated Fourier series. Then, the optimum values of the coefficients of the series are obtained through an optimization approach. The validation and the performance of the proposed structure were verified using some examples. It was observed that the designed polarizers have a good performance in the desired incidence angle range. Also, as the thickness of the polarizer is chosen larger or its desired relative incidence angle range is decreased, whose performance is increased. The proposed method can be extended for IPLs, whose magnetic permeability is inhomogeneous solely or along with their electric permittivity. Also, we can consider IPLs for spherical wavefronts instead of planar ones in the future.

REFERENCES

1. MacNeille, S. M., "Beam splitter," U. S. patent 2, 403, 731, July 9, 1946.
2. Mouchart, J., J. Begel, and E. Duda, "Modified MacNeille cube polarizer for a wide angular field," *Appl. Opt.*, Vol. 28, 2847–2853, 1989.
3. Monga, J. C., "Multilayer thin-film polarizers with reduced electric-field intensity," *J. Mod. Opt.*, Vol. 36, 769–784, 1989.
4. Li, L. and J. A. Dobrowolski, "Visible broadband, wide-angle, thin-film multilayer polarizing beam splitter," *Appl. Opt.*, Vol. 35, 2221–2225, 1996.
5. Thomsen, M. and Z. L. Wu, "Polarizing and reflective coatings based on half-wave layer pairs," *Appl. Opt.*, Vol. 36, 307–313, 1997.
6. Li, L. and J. A. Dobrowolski, "High-performance thin-film polarizing beam splitter operating at angles greater than the critical angle," *Appl. Opt.*, Vol. 39, 2754–2771, 2000.
7. Awasthi, S. K. and S. P. Ojha, "Wide-angle, broadband plate polarizer with 1D photonic crystal," *Progress In Electromagnetics Research*, PIER 88, 321–335, 2008.
8. Hecht, E., *Optics*, 4th edition, 349, Addison Wesley, 2002.
9. Dummer, D. J., S. G. Kaplan, L. M. Hanssen, A. S. Pine, and Y. Zong, "High-quality Brewster's angle polarizer for broadband infrared application," *Appl. Opt.*, Vol. 37, 1194–1204, 1998.
10. McCormick, F. B., F. A. P. Tooley, T. J. Cloonan, J. L. Brubaker, A. L. Lentine, R. L. Morrison, S. J. Hinterlong, M. J. Herron, S. L. Walker, and J. M. Sasian, "Experimental investigation of a free-space optical switching network by using symmetric selfelectro-optic-effect devices," *Appl. Opt.*, Vol. 31, 5431–5446, 1992.
11. Ojima, M., A. Saito, T. Kaku, M. Ito, Y. Tsunoda, S. Takayama, and Y. Sugita, "Compact magneto-optical disk for coded data storage," *Appl. Opt.*, Vol. 25, 483–489, 1986.
12. Kunstmann, P. and H. J. Spitschan, "General complex amplitude addition in a polarization interferometer in the detection of pattern differences," *Opt. Commun.*, Vol. 4, 166–168, 1971.
13. Zhang, J.-C., Y.-Z. Yin, and J.-P. Ma, "Multifunctional meander line polarizer," *Progress In Electromagnetics Research Letters*, Vol. 6, 55–60, 2009.
14. Huang, H., Y. Fan, B.-I. Wu, and J. A. Kong, "Tunable TE/TM wave splitter using a gyrotropic slab," *Progress In*

- Electromagnetics Research*, PIER 85, 367–380, 2008.
15. Bilotti, F., A. Toscano, and L. Vegni, “Very fast design formulas for microwave nonhomogeneous media filters,” *Microw. Opt. Tech. Letters*, Vol. 22, No. 3, 218–221, 1999.
 16. Vegni, L. and A. Toscano, “Full-wave analysis of planar stratified with inhomogeneous layers,” *IEEE Trans. Antennas and Propagation*, Vol. 48, No. 4, 631–633, April 2000.
 17. Toscano, A., L. Vegni, and F. Bilotti, “A new efficient method of analysis for inhomogeneous media shields and filters,” *IEEE Trans. Electromagn. Compat.*, Vol. 43, No. 3, 394–399, August 2001.
 18. Khalaj-Amirhosseini, M., “Wideband flat radomes using inhomogeneous planar layers,” *Int. Journal of Antennas and Propagation*, Vol. 2008, 869720–869725, 2008.
 19. Khalaj-Amirhosseini, M., “Using inhomogeneous planar layers as impedance matchers between two different mediums,” *Int. Journal of Microwave Science and Technology*, Vol. 2008, 869720, 1–5, 2008.
 20. Khalaj-Amirhosseini, M., “To analyze inhomogeneous planar layers by cascading thin linear layers,” *Progress In Electromagnetics Research B*, Vol. 3, 95–104, 2008.
 21. Khalaj-Amirhosseini, M., “Analysis of lossy inhomogeneous planar layers using finite difference method,” *Progress In Electromagnetics Research*, PIER 59, 187–198, 2006.
 22. Khalaj-Amirhosseini, M., “Analysis of lossy inhomogeneous planar layers using Taylor’s series expansion,” *IEEE Trans. Antennas and Propagation*, Vol. 54, No. 1, 130–135, January 2006.
 23. Khalaj-Amirhosseini, M., “Analysis of lossy inhomogeneous planar layers using fourier series expansion,” *IEEE Trans. Antennas and Propagation*, Vol. 55, No. 2, 489–493, February 2007.
 24. Khalaj-Amirhosseini, M., “Analysis of lossy inhomogeneous planar layers using equivalent sources method,” *Progress In Electromagnetics Research*, PIER 72, 61–73, 2007.
 25. Khalaj-Amirhosseini, M., “Analysis of lossy inhomogeneous planar layers using the method of moments,” *Journal of Electromagnetic Waves and Applications*, Vol. 21, No. 14, 1925–1937, 2007.
 26. Khalaj-Amirhosseini, M., “An approximated closed form solution for inhomogeneous planar layers,” *IET Proc. Microwaves, Antennas and Propagation*, Vol. 3, No. 6, 899–905, 2009.